Knævelsrud et al., http://www.jcb.org/cgi/content/full/jcb.201205129/DC1

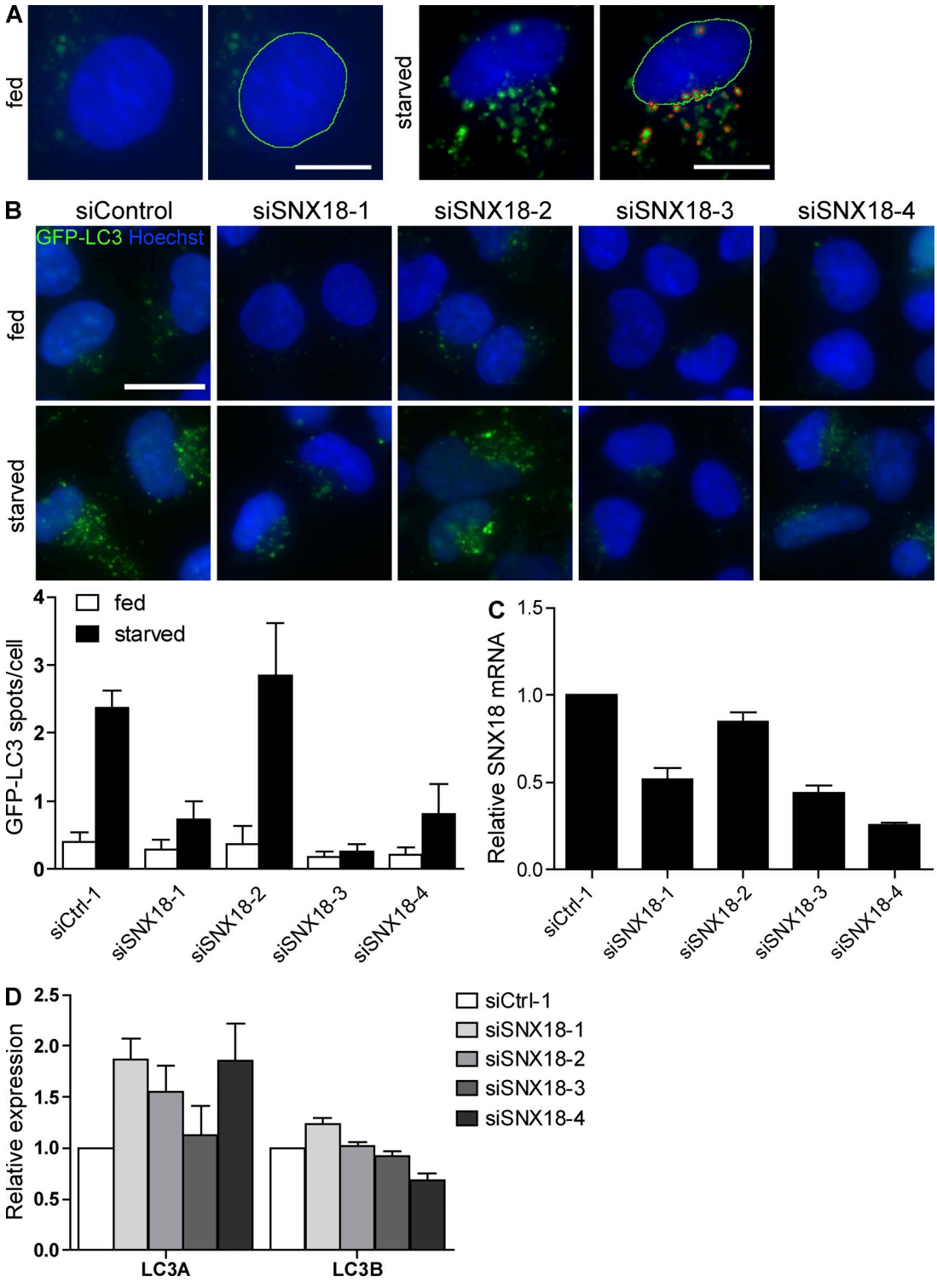

Figure S1. **The effect of SNX18 siRNA on GFP-LC3 spots correlates with SNX18 mRNA levels.** (A) Detection of GFP-LC3 spots by the Olympus ScanR software (detected nuclei delineated in green, detected spots in red). Note that only the strongest and most defined spots were detected. Bars, 5 µm. (B) HEK GFP-LC3 cells were separately transfected with the four different siRNA oligonucleotides of the SMARTpool against SNX18, and the number of GFP-LC3 spots/cell was quantified. The images for starved cells treated with siControl and siSNX18-3 are also shown in Fig. 1 C. Bars, 10 µm. The graphs show mean ± SEM (error bars), $n = 3$. (C) Relative expression of SNX18 mRNA corresponding to the images in B. The graph shows mean relative expression from two experiments performed in triplicate ± range (error bars). (D) Relative expression of LC3A and LC3B mRNA upon SNX18 knockdown, corresponding to B. The graph shows mean relative expression from two experiments performed in triplicate ± range (error bars).

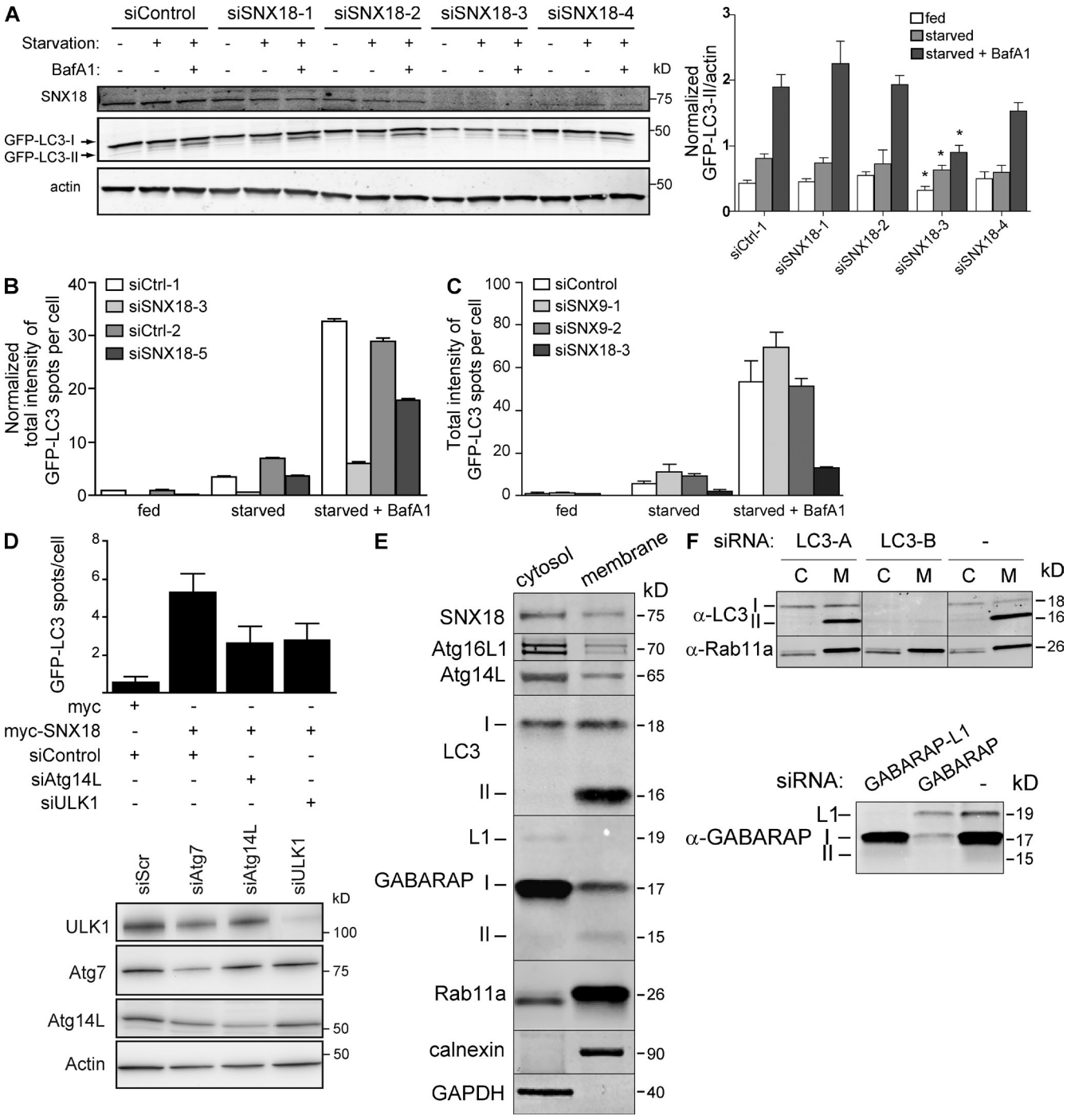

Figure S2. **SNX18, but not SNX9, is required for autophagosome formation.** (A) HEK GFP-LC3 cells were separately transfected with the four different siRNA oligonucleotides of the SMARTpool against SNX18 or the corresponding control and starved or not starved for 2 h in the presence or absence of BafA1. After lysis and separation by SDS-PAGE, Western blotting was performed to monitor GFP-LC3 lipidation and to confirm SNX18 protein knockdown. The graph shows quantification of the levels of GFP-LC3-II/actin (graph shows mean ± SEM [error bars], $n = 3$; *, $P < 0.05$ between siSNX18 and the corresponding siControl sample). (B) HEK GFP-LC3 cells were transfected with the indicated siRNA oligonucleotides and starved or not starved for 2 h in the presence or absence of BafA1. The total intensity of GFP-LC3 spots per cell for each condition was determined. The graph shows mean ± SEM (error bars), $n = 3$. (C) HEK GFP-LC3 cells were transfected with the indicated siRNA oligonucleotides against SNX9 or SNX18 and treated as in B. The graph shows mean ± SEM (error bars), $n = 3$, with a total of 1,500 cells. (D) HEK GFP-LC3 cells were transfected with the indicated siRNA oligonucleotides and then with myc-SNX18 or a myc control vector, followed by automated imaging and analysis of the number of GFP-LC3 spots per cell. The graph shows mean ± SEM (error bars), $n = 3$. Immunoblot analysis of knockdown is shown below. (E) Equal proportions of cytosol and membrane fractions from HeLa cells grown in full medium were analyzed by immunoblotting using antibodies against the indicated proteins. Analysis of calnexin and GAPDH validated the fractionation method and showed no cross-contamination between the fractions. Atg16L appeared as a doublet, which corresponds to two different splice forms present in HeLa cells as previously shown (Mizushima et al., 2003). (F) HeLa cells were transfected with siRNA against LC3-A, LC3-B, GABARAP, or GABARAP-L1, or left untreated (−), and after 72 h, membrane (M) and cytosol (C) were prepared (for LC3 analysis) or lysed (for GABARAP analysis), and analyzed by immunoblotting using the indicated antibodies. Black lines indicate that intervening lanes have been spliced out.

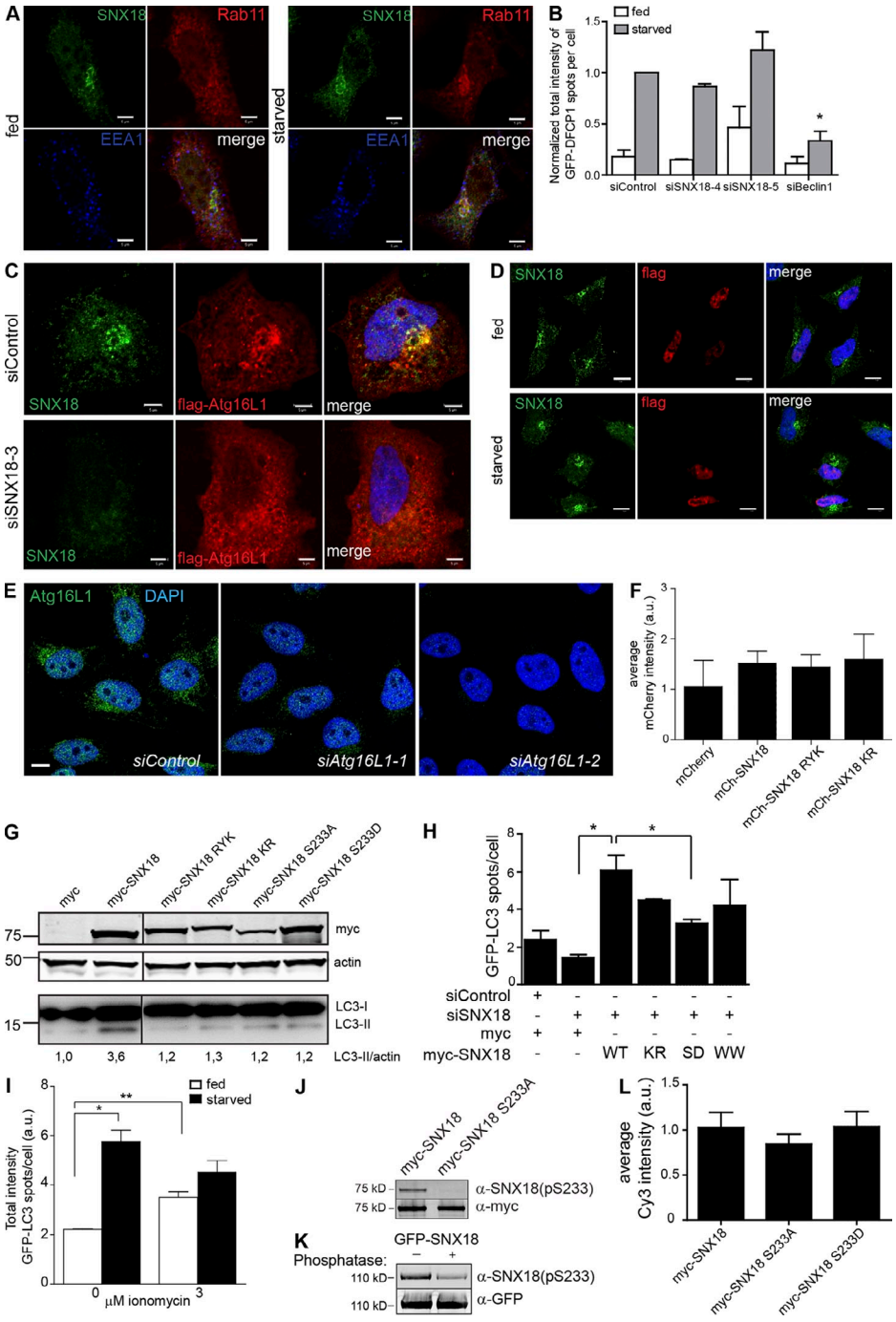

Figure S3. **SNX18 membrane binding and phosphorylation mutants.** (A) HeLa cells were grown in nutrient-rich medium (fed) or starved for 2 h before fixation and immunostaining against endogenous SNX18, Rab11, and EEA1. Bars, 5 µm. (B) HEK GFP-DFCP1 cells transfected with the indicated siRNAs were starved or not starved for 50 min. After fixation, the total intensity of GFP-DFCP1 spots per cell was quantified from 500 cells (graph shows mean ± SEM [error bars], $n = 3$). *, $P < 0.05$. (C) HeLa cells were transfected with control or SNX18 siRNA and later with flag-Atg16L1, followed by a 2-h incubation in nutrient-rich (fed) or starvation medium before immunostaining and confocal imaging. Bars, 5 µm. (D) HeLa cells were transfected with myc-SNX18 and a 3×flag control vector and then starved or not starved for 2 h before immunostaining with anti-myc and anti-flag antibodies and confocal microscopy analysis (control for Fig. 4 B). Bars, 10 µm. (E) HeLa cells were transfected with two different siRNA oligos against Atg16L1 or the corresponding control and immunostained with anti-Atg16L1 antibodies and analyzed by confocal microscopy. Bar, 5 µm. (F) HEK GFP-LC3 cells were transfected to overexpress the indicated mCherry-tagged SNX18 constructs for 16 h. The mean mCherry intensity was quantified as a control for equal expression levels (control for corresponding Fig. 4 D). (G) HEK GFP-LC3 cells were transfected to overexpress the indicated myc-tagged SNX18 constructs for 16 h. The ratio of LC3-II to actin, as determined by Western blotting, was quantified. Black lines indicate that intervening lanes have been spliced out. (H) HEK GFP-LC3 cells were transfected with control siRNA or siRNA against SNX18. The next day, they were transfected with siRNA-resistant plasmids encoding myc-SNX18 WT, or with mutations KR, S233D (SD) or W154S/W158S (WW). 1 d later, the number of GFP-LC3 spots per cell was quantified (mean ± SEM [error bars], $n = 3$; *, $P < 0.05$.) (I) HEK GFP-LC3 cells were starved or not starved for 2 h in the absence of presence of 3 µM ionomycin followed by automated imaging and analysis of the total intensity of GFP-LC3 spots per cell. The graph shows mean ± SEM (error bars), $n = 3$. *, $P < 0.05$; **, 0.01. (J) HeLa cells were transfected to overexpress myc-tagged full-length WT SNX18 (myc-SNX18) or mutant S233A (myc-SNX18 S233A) for 16 h, after which the cells were starved in EBSS for 90 min. Proteins were immunoprecipitated from lysates with anti-myc antibodies and analyzed by immunoblotting using phosphospecific SNX18 pS233 and myc antibodies. (K) GFP-Trap–enriched GFP-SNX18, obtained from cells starved for 90 min, was either mock-treated or treated with Lambda phosphatase and analyzed by immunoblotting using the phosphospecific SNX18 pS233 antibody. Anti-GFP shows equal amount of GFP-SNX18. (L) HEK GFP-LC3 cells were transfected to overexpress the indicated myc-tagged SNX18 constructs for 16 h, followed by immunostaining with an anti-myc antibody and a Cy3-labeled secondary antibody. The mean Cy3 intensity of was quantified as a control for equal expression levels in cells used to quantify the number of GFP-LC3 spots per cell (Fig. 5 C). The graph shows mean ± SEM (error bars).

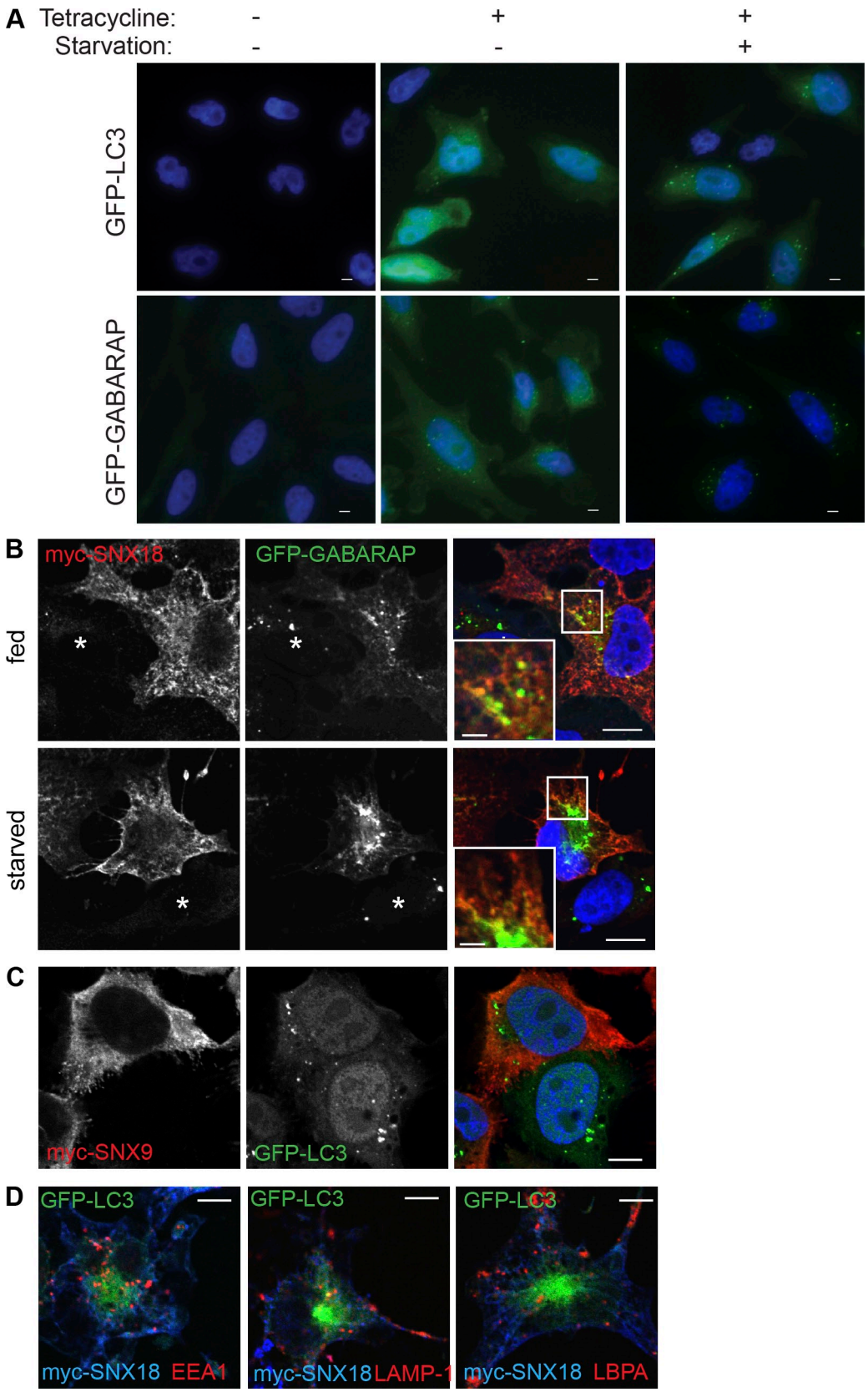

Figure S4. **myc-SNX18 induced GFP-LC3–positive membrane tubules.** (A) TRex FlpIN HeLa cells were stably transfected to express GFP-LC3 or -GABARAP under the control of a tetracycline-inducible promoter. (B) HeLa cells inducibly expressing GFP-GABARAP were transfected with a plasmid encoding myc-SNX18. The asterisks denote cells not expressing myc-SNX18. Insets show enlarged views of the boxed regions. (C) HeLa cells inducibly expressing GFP-LC3 were transfected with a plasmid encoding myc-SNX9. (D) HeLa cells inducibly expressing GFP-LC3 were transfected with a plasmid encoding myc-SNX18 and immunostained for the indicated proteins. Bars: (A) 5 µm; (B, main panels) 20 µm; (B, insets) 5 µm; (C and D) 10 µm.

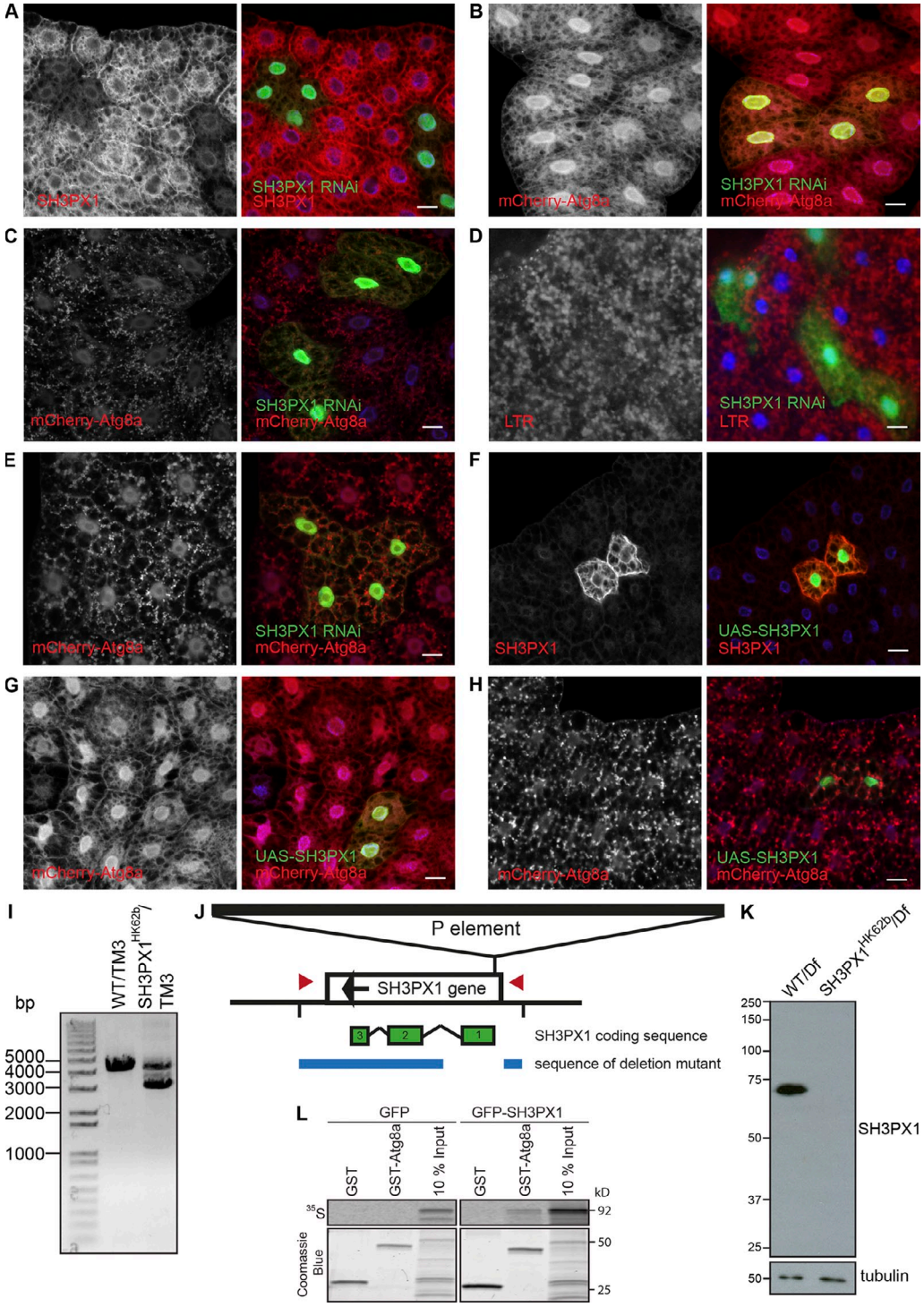

Figure S5. **SH3PX1 is necessary, but not sufficient for autophagosome formation.** (A) SH3PX1 protein levels are decreased by SH3PX1 RNAi. Fat bodies from third instar larvae expressing SH3PX1 RNAi (GFP-positive cells) were stained for endogenous SH3PX1. (B) Fat bodies from mCherry-Atg8a–expressing fed larvae with SH3PX1 RNAi clones (GFP positive). (C) SH3PX1 RNAi (GFP-positive cells) results in formation of smaller mCherry-Atg8a–marked autophagosomes after 3 h of starvation compared with WT cells. (D and E) LTR punctae (D) and mCherry-Atg8a–positive autophagosomes (E) are smaller in SH3PX1 RNAi clones (GFP-positive) compared with WT cells during developmental autophagy in 113-h-old larvae. (F) Fat body overexpressing SH3PX1 (GFP-positive cells) by actin-GAL4 through the UAS in the $SH3PX1^{EY08084}$ P element in the 5′ UTR of the SH3PX1 gene was stained for endogenous SH3PX1. (G and H) SH3PX1 overexpression does not induce or change formation of mCherry-positive autophagosomes in fat bodies from fed (G) or 3-h starved (H) larvae. Bars, 20 µm. Genotypes: (A and D) hsflp; UAS-dicer/+; Act>CD2>GAL4 UAS-GFPnls/UAS-SH3PX1 RNAi; (B, C, and E) hsflp; UAS-dicer/+; r4:mCherry-Atg8a Act>CD2>GAL4 UAS-GFPnls/UAS-SH3PX1 RNAi; (F) hsflp; +; Act>CD2>GAL4 UAS-GFPnls/UAS-SH3PX1; (G and H) hsflp; +; r4:mCherry-Atg8a Act>CD2>GAL4 UAS-GFPnls/UAS-SH3PX1. (I–K) The P element $SH3PX1^{EY08084}$ located in the 5′ UTR of the SH3PX1 gene was remobilized and lines where part of the gene region was deleted were screened by PCR. One such line missing 1,198 bp of the gene region was identified (I; $SH3PX1^{HK62b}$), and sequencing showed that the first exon of SH3PX1 including the start codon, was deleted (1,198 nucleotides removed from the EY08084 insertion site [3L:9,706,877; FlyBase release FB2012_02]). This is depicted in J as an overview of the SH3PX1 gene region with the inserted P element, the coding sequence, and the sequence still present in the deletion mutant. Primers for PCR amplification are indicated by red arrowheads. (K) Fat bodies from third instar larvae with indicated genotypes were dissected out and lysed in SDS sample buffer. Lysates were analyzed by Western blotting using the indicated antibodies. (L) GFP and GFP-tagged SH3PX1 were in vitro translated in reticulocyte lysate in the presence of [^{35}S]methionine and incubated with GST or GST-tagged DrAtg8a. The resulting pulldowns were separated by SDS-PAGE. Coomassie blue staining shows the presence of the GST proteins and the in vitro translated copurified proteins were detected by autoradiography.

Table S1. **Reagents and results for the primary screen**

Gene	Gene ID	Accession no.	GI no.	Dharmacon SMARTpool	No. of cells analyzed	GFP-LC3 spots per cell			
						Fed		Starved	
						Average	SD	Average	SD
SNX18	112574	NM_052870	16418370	L-013438-01	37,513	0.30	0.11	0.70	0.29
ULK1	8408	NM_003565	225637564	L-005049-01	393,570	0.43	0.17	1.00	0.28
RPS6KC1	26750	NM_012424	19923722	L-005371-00	52,785	0.61	0.12	1.82	0.46
PLD1	5337	NM_002662	46276864	L-009413-00	46,270	0.78	0.18	1.88	0.68
SNX4	8723	NM_003794	23111044	L-011520-00	48,435	0.63	0.11	2.01	0.87
SNX3	8724	NM_152827	23111040	L-011521-01	40,693	0.65	0.23	2.04	0.56
SNX2	6643	NM_003100	23111037	L-017520-00	53,688	0.74	0.14	2.16	0.77
SH3PXD2B	285590	NM_001017995	63055058	L-032834-01	39,858	0.66	0.11	2.11	0.11
SNX8	29886	NM_013321	23943857	L-014196-01	42,526	0.64	0.15	2.14	0.25
SNX25	83891	NM_031953	38708168	L-014761-01	44,557	0.68	0.14	2.15	0.34
SNX27	81609	NM_030918	73695940	L-017346-01	52,888	0.65	0.13	2.17	0.91
PXK	54899	NM_017771	31543451	L-005367-00	49,517	0.66	0.12	2.22	0.32
SNX19	399979	NM_014758	7662025	L-029832-01	32,791	0.65	0.23	2.23	0.26
PLD2	5338	NM_002663	20070140	L-005064-00	53,258	0.57	0.20	2.30	0.75
SNX12	29934	NM_013346	23111029	L-013648-00	38,114	0.68	0.05	2.31	0.35
SNX9	51429	NM_016224	23111056	L-017335-00	43,436	0.53	0.10	2.34	0.44
SNX16	64089	NM_152837	23238247	L-013044-01	46,089	0.74	0.28	2.36	0.60
SNX7	51375	NM_152238	23111054	L-013216-01	54,382	0.82	0.32	2.38	0.80
PIK3C2A	5286	NM_002645	4505798	L-006771-00	37,354	0.65	0.11	2.40	0.55
SNX21	90203	NM_152897	23510349	L-013643-01	32,791	0.58	0.20	2.43	0.33
KIF16b	55614	NM_024704	41327690	L-009495-00	55,651	0.74	0.22	2.49	0.95
SH3PXD2a	9644	NM_014631	55749543	L-006657-00	39,858	0.77	0.15	2.51	0.16
NISCH	11188	NM_007184	66472381	L-019677-00	52,259	0.84	0.24	2.52	0.55
CISK	23678	NM_170709	25168266	L-004162-00	70,157	0.63	0.27	2.53	0.46
SNX5	27131	NM_014426	23111045	L-012524-00	48,111	0.68	0.13	2.54	0.84
SNX10	29887	NM_013322	23111022	L-017559-01	47,895	0.68	0.13	2.55	0.63
LOC64654/ SNX30	401548	XM_945049	89030537	L-029584-01	50,950	0.81	0.20	2.55	0.16
SNX11	29916	NM_013323	23111025	L-013673-01	42,716	0.85	0.19	2.57	0.63
NCF4	4689	NM_000631	47519797	L-011128-01	48,168	0.80	0.16	2.59	0.53
SNX13	23161	NM_015132	87196349	L-009381-01	43,526	0.69	0.27	2.61	0.85
NCF1	4687	NM_000265	4557784	L-009958-00	33,652	0.74	0.05	2.62	0.52
SNX33	257364	NM_153271	23397573	L-015876-00	31,301	0.84	0.21	2.63	0.47
SNX17	9784	NM_014748	23238249	L-013427-01	49,559	0.76	0.36	2.67	0.64
SNX15	29907	NM_147777	46370088	L-017488-01	33,420	0.88	0.20	2.69	0.39
LOC646564	646564	XM_929500	89040212	L-037482-00	50,634	0.71	0.14	2.72	0.60
SNX22	79856	NM_024798	71772837	L-014452-01	49,639	0.87	0.50	2.77	0.37
SNX20	124460	NM_182854	33504570	L-016514-01	33,349	0.98	0.17	2.84	0.40
SNX1	6642	NM_148955	71772739	L-017518-00	34,301	0.80	0.23	2.85	0.25
HS1BP3	64342	NM_022460	68800429	L-013029-01	36,266	0.89	0.20	2.92	0.27
SNX24	28966	NM_014035	7662654	L-020568-01	48,714	0.98	0.26	2.92	0.81
SNX31	169166	NM_152628	24432084	L-016021-01	33,547	0.76	0.27	2.98	0.54
SNX14	57231	NM_020468	39777615	L-013190-01	33,568	0.60	0.20	3.07	0.37
TSG101	7251	NM_006292	18765712	L-003549-00	67,115	1.22	0.43	3.79	0.96
Non-targeting 1[a]					92,798	0.63	0.13	2.79	0.46
Non-targeting 2[b]					81,587	0.75	0.14	2.81	0.54
Non-targeting 3[c]					82,485	0.81	0.81	0.81	0.81

A comprehensive list of the gene targets, siRNA numbers, number of cells analyzed, and GFP-LC3 spots per cell (average and SD for fed and starved cells) from the primary screen. The siRNA treatments did not significantly affect cell proliferation as judged by limited variation in the total number of cells detected on the 100 images analyzed from each siRNA treatment.
[a]ON-TARGET plus Non-targeting Pool.
[b]siGENOME Non-targeting Pool.
[c]siGENOME Non-targeting Pool #2.

Table S2. **Reagents and results for the secondary screen**

Gene	Dharmacon ON target plus	siRNA sequence (5′–3′)	Percent knockdown of mRNA	No. of cells analyzed	GFP-LC3 spots			
					Fed		Starved	
					Average	SD	Average	SD
SNX18	J-013438-09[a]	AGAGCAAGAUAGACGGCUU	50	35,495	0.29	0.15	0.73	0.28
	J-013438-10[b]	GAGCAUACCCGGACCUCGA	0	61,436	0.38	0.26	2.85	0.77
	J-013438-11[c]	GCGGAGAAGUUCCCGGUCA	60	51,626	0.18	0.08	0.26	0.12
	J-013438-12[d]	CGGACAUCAUCCACGUUCA	70	37,378	0.22	0.11	0.82	0.44
ULK1	J-005049-05	CAGCAUCACUGCCGAGAGG	65	98,195	0.37	0.13	1.46	0.22
	J-005049-06	CCACGCAGGUGCAGAACUA	65	81,939	0.26	0.15	0.39	0.12
	J-005049-07	GCACAGAGACCGUGGGCAA	50	89,098	0.45	0.09	2.47	0.50
	J-005049-08	UCACUGACCUGCUCCUUAA	70	87,029	0.27	0.13	0.91	0.30
SNX14	J-013190-09	UGAAAUUUCUGCUGUGCGA	63	52,135	0.52	0.35	2.82	1.09
	J-013190-10	AGAUACUACCAGAUGUAAA	61	53,533	0.45	0.28	2.66	1.15
	J-013190-11	GUUAGGACUUCAGGAAUUA	77	49,324	0.36	0.19	2.28	0.92
	J-013190-12	CAUUAAUUCUUGUGAGUCU	65	44,819	0.43	0.27	1.28	0.32
RPS6KC1	J-005371-06	GGAAUUGUGUGCCGCGAUU	83	43,775	0.47	0.05	3.36	0.50
	J-005371-07	CAGCUCAGAUCCUAAGUUU	77	49,744	0.45	0.09	3.23	0.44
	J-005371-08	GGAGAUAUGUCUUUGUUAC	77	52,173	0.37	0.07	2.58	0.30
	J-005371-09	GGAAUAAAUACUCACACUA	64	35,236	0.24	0.06	0.64	0.12
PLD1	J-009413-05	CAACAGAGUUUCUUGAUAU	83	44,274	0.35	0.05	2.74	0.32
	J-009413-06	GGUAAUCAGUGGAUAAAUU	73	46,204	0.53	0.07	2.70	0.44
	J-009413-07	CCAUGGAGGUUUGGACUUA	73	45,901	0.31	0.07	1.62	0.34
	J-009413-08	CCGGGUAUAUGUCGUGAUA	53	50,080	0.46	0.08	2.94	0.30
SNX31	J-016021-09	ACAGAGUAUUAGAAUCGAA	30	47,529	0.34	0.05	2.80	0.33
	J-016021-10	GCAGAUUGAAGUUCCGGAA	51	47,439	0.46	0.06	3.05	0.53
	J-016021-11	GUCGAGAGCUCUUGGGCUA	34	34,578	0.52	0.06	3.34	0.62
	J-016021-12	AGGUACGGCACUAUGGAUA	46	48,243	0.43	0.05	2.77	0.58
SNX24	J-020568-09	GAAAAGAGAUACAGCGAAU	81	54,686	0.43	0.34	2.39	0.94
	J-020568-10	CUUGGAACAGCGACGACAA	64	46,423	0.97	0.73	5.24	1.98
	J-020568-11	GCCAAGUGUUUAAGAAGUA	80	45,944	0.34	0.26	2.05	1.58
	J-020568-12	GCGUAGAAACCCAUGAAAA	76	51,801	0.32	0.25	2.15	1.29
SNX20	J-016514-09	CGUUCAGGGAGGAGAUCGA	0	41,356	0.42	0.09	2.07	0.38
	J-016514-10	GCAAGGACUUCGUGACUCU	0	34,956	0.71	0.20	3.34	0.89
	J-016514-11	GCUGGAAGCACGUCAAACU	3	27,247	0.87	0.23	2.92	0.61
	J-016514-12	UCUCUAAGUUUGUGGUGUA	3	48,282	0.46	0.09	3.27	0.48
HS1BP3	J-013029-09	AAGAAGGAGUGACCGGUAU	67	51,365	0.60	0.40	4.14	1.05
	J-013029-10	UGAAGAGGCUUUCGACUUU	97	50,411	0.69	0.47	4.08	1.13
	J-013029-11	GAGCCUGAAGGGCGAGGAU	65	48,866	0.94	0.67	7.07	1.54
	J-013029-12	UCCCAAAGUGGCCGUGAAA	0	56,401	0.46	0.41	2.47	0.89
Non-targeting	D-001810-01[e]		0	199,315	0.41	0.13	2.37	0.26

Listing the gene targets, siRNA numbers and sequences, percent knockdown of mRNA for the specified target, number of cells analyzed, and GFP-LC3 spots per cell (average and SD for fed and starved cells) from the secondary screen. Names used in figures are defined by footnotes.
[a]siSNX18-1.
[b]siSNX18-2.
[c]siSNX18-3.
[d]siSNX18-4.
[e]siCtrl-1.

Table S3. **Plasmids used in this study**

Plasmid	Primer sequences	Reference
pCMVmycSNX18		Håberg et al., 2008
pCMVmycSNX18 RYK constructed by mutagenesis using the primers listed in the next column	5′-GCAGGTGCCGGTGCATCGGCAGGCCGCGCACTTCGACTGGCTGTACG-3′ and 5′-CGTACAGCCAGTCGAAGTGCGCGGCCTGCCGATGCACCGGCACCTGC-3′	This study
pCMVmycSNX18 KR constructed by mutagenesis using the primers listed in the next column	5′-GCCTGGAAGCAGGGCGAGGAGAAGGCCGAGAAGGA-3′ and 5′-TCCTTCTCGGCCTTCTCCTCGCCCTGCTTCCAGGC-3′	This study
pCMVmycPX-BAR		Håberg et al., 2008
pCMVmycPX-BAR S233A constructed by mutagenesis using the primers listed in the next column	5′-CAATCGCTTCGCCACCTTCGTCAAG-3′and 5′-CTTGACGAAGGTGGCGAAGCGATTG-3′	This study
pCMVmycPX-BAR S233D constructed by mutagenesis using the primers listed in the next column	5′-CCTCAATCGCTTCGACACCTTCGTCAAG-3′ and 5′-CTTGACGAAGGTGTCGAAGCGATTGAGG-3′	This study
pCMVmycSNX18 S233A constructed by mutagenesis using the primers listed in the next column	5′-CAATCGCTTCGCCACCTTCGTCAAG-3′and 5′-CTTGACGAAGGTGGCGAAGCGATTG-3′	This study
pCMVmycSNX18 S233D constructed by mutagenesis using the primers listed in the next column	5′-CCTCAATCGCTTCGACACCTTCGTCAAG-3′ and 5′-CTTGACGAAGGTGTCGAAGCGATTGAGG-3′	This study
pCMVmycSNX18 W154S/W158S constructed by mutagenesis using the primers listed in the next column	5′-GCAGCGATGATGACTCGGACGACGAGTGGGA-3′ and 5′-TCCCACTCGTCGTCCGAGTCATCATCGCTCC-3′ then 5′-ACTCGGACGACGAGTCGGACGACAGCTCCAC-3′ and 5′-GTGGAGCTGTCGTCCGACTCGTCGTCCGAGT-3′	This study
pDESTmyc SNX18 WT siSNX18 3 resistant constructed by mutagenesis of pENTR SNX18 using the primers listed in the next column	5′-GCGCGCCTGGCGGAAAAATTTCCTGTCATCTCCGTGCCC-3′ and 5′-GGGCACGGAGATGACAGGAAATTTTTCCGCCAGGCGCGC-3′	This study
pDESTmyc SNX18 KR siSNX18 3 resistant constructed by mutagenesis of pENTR SNX18 KR using the primers listed in the next column	5′-GCGCGCCTGGCGGAAAAATTTCCTGTCATCTCCGTGCCC-3′ and 5′-GGGCACGGAGATGACAGGAAATTTTTCCGCCAGGCGCGC-3′	This study
pDESTmyc SNX18 S233D siSNX18 3 resistent constructed by mutagenesis of pENTR SNX18 S233D using the primers listed in the next column	5′-GCGCGCCTGGCGGAAAAATTTCCTGTCATCTCCGTGCCC-3′ and 5′-GGGCACGGAGATGACAGGAAATTTTTCCGCCAGGCGCGC-3′	This study
pDESTmyc SNX18 W154S/W158S siSNX18 3 resistent constructed by mutagenesis of pENTR SNX18 W154S/W158S using the primers listed in the next column	5′-GCGCGCCTGGCGGAAAAATTTCCTGTCATCTCCGTGCCC-3′ and 5′-GGGCACGGAGATGACAGGAAATTTTTCCGCCAGGCGCGC-3′	This study
pEGFPAtg14L		Addgene plasmid 21635 Matsunaga et al., 2009
pDEST53-p62		Pankiv et al., 2007
pDEST53-SNX18 Constructed by subcloning from pCMVmycSNX18 (Håberg et al., 2008) into pENTR and subsequent Gateway cloning into pDEST53 (Invitrogen)		This study
pDEST53-SNX18 SH3-LC Constructed by restriction digest of pENTR SNX18 and subsequent Gateway cloning into pDEST53		This study
pDEST53-SNX18 PX-BAR Constructed by subcloning from pCMVmycSNX18 (Håberg et al., 2008) into pENTR and subsequent Gateway cloning into pDEST53		This study
pDEST15-LC3A		Pankiv et al., 2007
pDEST15-LC3B		Pankiv et al., 2007
pDEST15-LC3C Constructed by subcloning from pGEX-4T-1-LC3C (Kirkin et al., 2009), provided by I. Dikic (Goethe University Medical School, Frankfurt Am Main, Germany), into pENTR and subsequent Gateway cloning into pDEST15 (Invitrogen)		This study
pDEST15-GABARAP		Pankiv et al., 2007
pDEST15-GABARAPL1		Pankiv et al., 2007

Table S3. **Plasmids used in this study** *(Continued)*

Plasmid	Primer sequences	Reference
pDEST15-GABARAPL2		Pankiv et al., 2007
pDEST EGFP LC3 G120A Constructed by Gateway cloning from pENTR LC3 G120A (constructed by A. Jain and obtained as a gift from T. Johansen) into pDEST EGFP		This study
mCFP-FRB		Varnai et al., 2006
mRFP-FKBP		Varnai et al., 2006
mRFP-FKBP-5pase		Varnai et al., 2006
pDEST15-Atg8a Constructed by Gateway cloning from pENTR DmAtg8a, provided by T. Johansen, into pDEST15		
pDEST53-SH3PX1 Constructed by subcloning from pOT2 SH3PX1, received through the Drosophila Genomics Resource Center (Stapleton et al., 2002), into pENTR and subsequent Gateway cloning into pDEST15 (Invitrogen)		This study

References

Håberg, K., R. Lundmark, and S.R. Carlsson. 2008. SNX18 is an SNX9 paralog that acts as a membrane tubulator in AP-1-positive endosomal trafficking. *J. Cell Sci.* 121:1495–1505. http://dx.doi.org/10.1242/jcs.028530

Kirkin, V., T. Lamark, Y.S. Sou, G. Bjørkøy, J.L. Nunn, J.A. Bruun, E. Shvets, D.G. McEwan, T.H. Clausen, P. Wild, et al. 2009. A role for NBR1 in autophagosomal degradation of ubiquitinated substrates. *Mol. Cell.* 33:505–516. http://dx.doi.org/10.1016/j.molcel.2009.01.020

Matsunaga, K., T. Saitoh, K. Tabata, H. Omori, T. Satoh, N. Kurotori, I. Maejima, K. Shirahama-Noda, T. Ichimura, T. Isobe, et al. 2009. Two Beclin 1-binding proteins, Atg14L and Rubicon, reciprocally regulate autophagy at different stages. *Nat. Cell Biol.* 11:385–396. http://dx.doi.org/10.1038/ncb1846

Mizushima, N., A. Kuma, Y. Kobayashi, A. Yamamoto, M. Matsubae, T. Takao, T. Natsume, Y. Ohsumi, and T. Yoshimori. 2003. Mouse Apg16L, a novel WD-repeat protein, targets to the autophagic isolation membrane with the Apg12-Apg5 conjugate. *J. Cell Sci.* 116:1679–1688. http://dx.doi.org/10.1242/jcs.00381

Pankiv, S., T.H. Clausen, T. Lamark, A. Brech, J.A. Bruun, H. Outzen, A. Øvervatn, G. Bjørkøy, and T. Johansen. 2007. p62/SQSTM1 binds directly to Atg8/LC3 to facilitate degradation of ubiquitinated protein aggregates by autophagy. *J. Biol. Chem.* 282:24131–24145. http://dx.doi.org/10.1074/jbc.M702824200

Stapleton, M., J. Carlson, P. Brokstein, C. Yu, M. Champe, R. George, H. Guarin, B. Kronmiller, J. Pacleb, S. Park, et al. 2002. A *Drosophila* full-length cDNA resource. *Genome Biol.* 3:RESEARCHH0080. http://dx.doi.org/10.1186/gb-2002-3-12-research0080

Varnai, P., B. Thyagarajan, T. Rohacs, and T. Balla. 2006. Rapidly inducible changes in phosphatidylinositol 4,5-bisphosphate levels influence multiple regulatory functions of the lipid in intact living cells. *J. Cell Biol.* 175:377–382. http://dx.doi.org/10.1083/jcb.200607116